CHIP28 Water Channels Are Localized in Constitutively Water-permeable Segments of the Nephron

Søren Nielsen,* Barbara L. Smith,‡ Erik Ilsø Christensen,* Mark A. Knepper,§ and Peter Agre‡

*Department of Cell Biology, Institute of Anatomy, University of Aarhus, DK-8000 Aarhus C, Denmark; ‡Departments of Medicine and Cell Biology/Anatomy, Johns Hopkins University School of Medicine, Baltimore, Maryland 21205; and §Laboratory of Kidney and Electrolyte Metabolism, National Heart, Lung and Blood Institute, National Institutes of Health, Bethesda, Maryland 20892

Abstract. The sites of water transport along the nephron are well characterized, but the molecular basis of renal water transport remains poorly understood. CHIP28 is a 28-kD integral protein which was proposed to mediate transmembrane water movement in red cells and kidney (Preston, G. M., T. P. Carroll, W. B. Guggino, and P. Agre. 1992. *Science [Wash. DC]*. 256:385–387). To determine whether CHIP28 could account for renal epithelial water transport, we used specific polyclonal antibodies to quantitate and localize CHIP28 at cellular and subcellular levels in rat kidney using light and electron microscopy. CHIP28 comprised 3.8% of isolated proximal tubule brush border protein. Except for the first few cells of the S1 segment, CHIP28 was immunolocalized throughout the convoluted and straight proximal tubules where it was observed in the microvilli of the apical brush border and in basolateral membranes. Very little CHIP28 was detected in endocytic vesicles or other intracellular structures in proximal tubules. Uninterrupted, heavy immunostaining of CHIP28 was also observed over both apical and basolateral membranes of descending thin limbs, including both short and long loops of Henle. These nephron sites have constitutively high osmotic water permeabilities. CHIP28 was not detected in ascending thin limbs, thick ascending limbs, or distal tubules, which are highly impermeable to water. Moreover, CHIP28 was not detected in collecting duct epithelia, where water permeability is regulated by antidiuretic hormone. These determinations of abundance and structural organization provide evidence that the CHIP28 water channel is the predominant pathway for constitutive transepithelial water transport in the proximal tubule and descending limb of Henle's loop.

THE mammalian kidney is a unique organ composed of discrete renal tubule segments which function together to permit the regulated excretion of water and solutes. Despite extensive knowledge of the sites of water transport along the renal tubule (reviewed by Knepper and Rector, 1991), the molecular basis of transmembrane water movement is poorly understood. The work of several laboratories suggests that transmembrane water flow occurs through water-selective channels located in specific segments of the nephron (reviewed by Finkelstein, 1987; Verkman, 1989). Large volumes of glomerular ultrafiltrate are believed to be reabsorbed through constitutively functional water-selective channels in the proximal tubule and the descending thin limb (Fig. 1). The subsequent segments, the ascending thin and thick limbs and the distal convoluted and connecting tubule, are all highly impermeable to water. The effluent from multiple nephrons empties into collecting ducts which are relatively impermeable to water unless stimulated with anti-diuretic hormone (ADH)[1]. ADH interacts with specific receptors on collecting duct epithelia which initiates a chain of events leading to insertion of water-selective channels in the apical plasma membrane (reviewed by Handler, 1988; Harris et al., 1991; Brown, 1991).

The structural identification of renal water channels is necessary to understand how they function. The first identified water channel protein is CHIP28 (Preston and Agre, 1991; Preston et al., 1992). CHIP28 is an abundant integral protein in human and rat red cells and kidney (Denker et al., 1988). Similarities between CHIP28 and membrane channels were recognized, hence "CHIP28," an acronym for CHannel forming Integral membrane Protein of 28 kD. The native CHIP28 protein is apparently a tetramer composed of three identical M_r 28-kD polypeptide subunits and a fourth which contains one or two large N-linked glycans and exhibits an apparent mobility of M_r 40–60 kD (Smith and Agre, 1991). The cDNA for CHIP28 was isolated and found to be homologous to the major intrinsic protein of mammalian lens (MIP26, Gorin et al., 1984) and other members of a family of membrane proteins with incompletely defined functions from diverse organisms (Preston and Agre, 1991). Recent studies have demonstrated that in-

1. *Abbreviations used in this paper:* ADH, anti-diuretic hormone; CHIP28, channel forming integral membrane protein of 28 kD.

jection of CHIP28 cRNA into *Xenopus* oocytes results in expression of a mercury-sensitive osmotic water pathway (Preston et al., 1992). Furthermore, synthetic liposomes reconstituted with purified CHIP28 protein exhibit classically-defined water channel activity (Zeidel et al., 1992).

The relationship between CHIP28 and renal water transport remains unclear, but several specific questions can now be answered. Is red cell CHIP28 the same molecule as the constitutively functional water channel in renal proximal tubules or the ADH-sensitive water channel in renal collecting ducts? Is CHIP28 present in both the apical and basolateral membranes of water-permeable renal epithelia as is necessary to explain the complete route of transcellular water flow? Can renal CHIP28 explain the magnitude of water reabsorption in the kidney which is at least 10 times the extracellular fluid volume per day? Immunolocalization was undertaken to define the cellular and subcellular organization of CHIP28 within rat kidney to answer these questions and thereby gain insight into the function of this protein.

Materials and Methods

Materials

Anticoagulated human red cells were obtained from the American Red Cross (Baltimore, MD). Reagent grade chemicals were from J. T. Baker (Phillipsburg, NJ). Electrophoresis supplies including SDS, acrylamide, TEMED, nitrocellulose blot, and silver reagent were from Bio-Rad Laboratories (Richmond, CA). Except where noted, other detergents and reagents were from Sigma Chemical Co. (St. Louis, MO).

Purification of CHIP28 Protein

CHIP28 was purified by a method derived from Smith and Agre (1991). Washed red cells from two units of human blood were lysed in 7.5 mM sodium phosphate (pH 7.4), and membrane vesicles were extracted with 1 M potassium iodide as described (Bennett, 1983). Extracted membrane vesicles from 400 ml of red cells were further extracted by shaking for 1 h at 22°C in 800 ml 1% (w/v) N-lauroylsarcosine, 1 mM NH_4HCO_3, 1 mM NaN_3, 1 mM dithiothreitol, and 0.5 mM phenylmethanesulfonyl fluoride and centrifuged 4 h at 31,000 *g* in a Beckman JA-14 rotor (Beckman Instruments, Fullerton, CA). The pellet was washed once in 7.5 mM sodium phosphate (pH 7.4) and solubilized by shaking for 1 h at 22°C in 1.2 liter of buffer A [20 mM Tris-HCl (pH 7.8), 1 mM NaN_3, 1 mM dithiothreitol] also containing 4% Triton X-100. After a 4-h centrifugation at 4°C the supernatant was filtered through 0.22 μm Millex GV membranes (Millipore Corp., Bedford, MA). Aliquots corresponding to 33 ml of packed red cells were adsorbed onto a 4.6 × 10 mm POROS Q/H anion-exchange column (PerSeptive Biosystems, Cambridge, MA) running at 3 ml/min with buffer A also containing 0.1% Triton X-100. The column was eluted with a 0.2–0.6 M NaCl gradient. The major A_{280} peak ran at 0.3 M NaCl, and these fractions were diluted with 5 vol of buffer A and rechromatographed in aliquots corresponding to 50 ml of packed red cells. The peak fractions from the second elution were then combined and electrophoresed through preparative 5 cm SDS-PAGE columns containing 12% acrylamide (Laemmli, 1970) using a Model 491 Prep Cell (Bio-Rad Laboratories). Elution was monitored by SDS-PAGE with silver staining; nonglycosylated CHIP28 (M_r 28 kD) was completely separated from glycosylated CHIP28 (M_r 40–60 kD).

Preparation and Characterization of Antibodies

Fractions containing the nonglycosylated CHIP28 protein were pooled for rabbit immunizations. Purified CHIP28 was mixed with Freund's complete adjuvant, and 1 wk after prebleeding, four young New Zealand white rabbits were injected with up to 100 μg of purified CHIP28 protein at multiple intradermal and subcutaneous sites. 4 wk after the initial immunization, the rabbits were boosted with 30 μg of purified CHIP28 in Freund's incomplete adjuvant. The rabbits were boosted at two week intervals thereafter until crop bleedings. Immunization of rabbits with an albumin-conjugated synthetic peptide corresponding to the NH_2-terminus of CHIP28 was described (Smith and Agre, 1991). The rabbit sera were incubated at 60°C for 30 min, diluted with equal vol of 150 mM NaCl, 10 mM sodium phosphate (pH 7.4), 1 mM NaEDTA, 1 mM NaN_3, 0.5 mM phenylmethanesulfonyl fluoride, 0.2% Triton X-100, and filtered through 0.22 μm Millex GV filters (Millipore Corp., Bedford, MA).

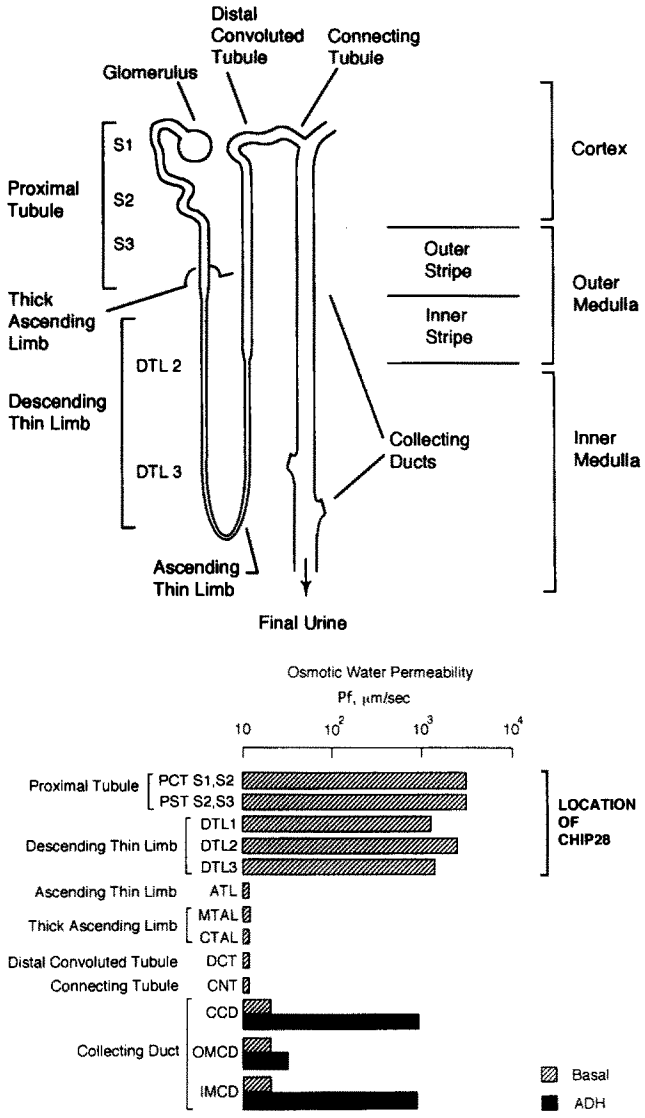

Figure 1. Diagram of mammalian nephron and compilation of water permeability measurements of nephron segments. (*Top*) Configuration of a long looped nephron. (A short looped nephron would descend to the transition between the outer and inner medulla [not shown]). (*Bottom*) Osmotic water permeability (P_f, μm/s) from published studies: *PCT*, rat proximal convoluted tubule (Green and Giebisch, 1989); *PST*, rabbit proximal straight tubule (Schafer et al., 1978); *DTL1*, hamster short descending thin limb (Imai, 1984); *DTL2,3* and *ATL*, chinchilla long descending thin limbs and ascending thin limbs (Chou and Knepper, 1992); *MTAL*, rabbit medullary thick ascending limb (Rocha and Kokko, 1973); *CTAL*, rabbit cortical thick ascending limb (Burg and Green, 1973); DCT, rabbit distal convoluted tubule (Gross and Kokko, 1975); *CNT*, rabbit connecting tubule (Imai, 1979); *CCD*, rat cortical collecting duct (Reif et al., 1984); *OMCD*, rabbit outer medullary collecting duct (Horster and Zink, 1982); *IMCD*, rat inner medullary collecting duct (Lankford et al., 1991; Chou et al., 1990).

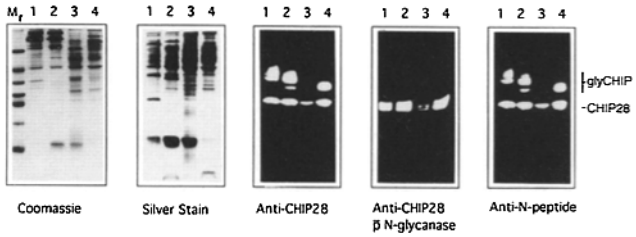

Figure 2. SDS-PAGE and immunoblots of membranes from red cells and renal cortex. Mol markers were of 66, 45, 36, 29, 24, 20, and 14 kD. A 5-μg aliquot of membrane protein was analyzed in each lane (see Methods): human red cells (lane *1*), rat red cells (lane *2*), total membranes from rat renal cortex (lane *3*), and brush border membrane vesicles from rat renal cortex (lane *4*). Identical SDS-PAGE slabs were stained with Coomassie or silver reagents. Immunoblots of these membranes were reacted with anti-CHIP28 or anti-N-peptide. (Note, the signal from glycosylated CHIP28 in total membranes from renal cortex [lane *3*] was lost during contact printing due to relatively low abundance of CHIP28 in these membranes). Before SDS-PAGE, identical membrane fractions were incubated with N-glycanase and reacted with anti-CHIP28 (shown) or anti-N-peptide (not shown).

A CHIP28 affinity column was prepared from purified, denatured CHIP28 from which the M_r 40–60 kD glycosylated CHIP28 subunits had been removed by preparative SDS-PAGE (above). Approximately 700 μg of purified CHIP28 protein was concentrated to 3 ml in 20 mM sodium phosphate (pH 7.4), 1 mM NaN_3, 0.1% (w/v) SDS using Centricon 10 microconcentrators (Amicon, Beverly, MA). 3 ml of Affi-Gel 15 agarose beads (Bio-Rad Laboratories) were washed and added to the CHIP28 concentrate and rocked gently for 18 h at 4°C. Unreacted sites were then blocked by addition of 1 M ethanolamine HCl (pH 8.0) for 1 h. The beads were then washed with 7.5 mM sodium phosphate (pH 7.4), 1 mM NaN_3, 0.1% (w/v) SDS and packed into two 7-mm diam columns. The columns were each sequentially washed with >50 vol of buffer B [0.1 M glycine, 2 M urea, 0.2% Triton X-100], then 1 M acetic acid, and finally with buffer C (150 mM NaCl, 50 mM sodium phosphate [pH 7.4], 1 mM NaEDTA, 1 mM NaN_3, 0.2% [v/v] Triton X-100).

"Anti-CHIP28" was affinity purified from the sera of rabbits immunized with nonglycosylated CHIP28 protein (described above). "Anti-N-peptide" was affinity purified from the sera of rabbits immunized with a synthetic peptide corresponding to the NH_2-terminus of CHIP28. (Note that the specificities of the antisera were previously reported [Smith and Agre, 1991]). The antisera were separately loaded onto the two affinity columns at 3 ml/h at 4°C which were then washed at 10 ml/h with 5 column volumes of buffer C, 5 column volumes of buffer B followed by a wash with ~10 column volumes 500 mM NaCl, 20 mM sodium phosphate (until A_{280} was zero), and a final wash with 5 column volumes of 50 mM sodium acetate (pH 5.0). The columns were eluted with 1 M acetic acid. The A_{280} was monitored and peaks were dialyzed against 150 mM NaCl, 50 mM sodium phosphate (pH 7.4), 1 mM NaEDTA, 1 mM NaN_3, concentrated against polyethylene glycol (PEG 8000, Fisher Scientific Co., Pittsburgh, PA), and again dialyzed.

Preparation of Membranes

Membranes were prepared from human and rat red cells by hypotonic lysis in 7.5 mM sodium phosphate (pH 7.4), 1 mM NaEDTA, 0.5 mM phenylmethanesulfonyl fluoride as described (Bennett, 1983). Kidneys were removed from sacrificed 200 gm Sprague Dawley rats, and the cortex was dissected. Total renal cortex membranes were prepared by homogenization in a Potter Elvehjem apparatus with removal of cytoplasm and organelles by lowspeed centrifugation; brush border membrane vesicles were prepared by serial centrifugations after addition of $MgSO_4$ as described (Mürer and Gmaj, 1986). Protein concentrations were determined with the BCA protein assay (Pierce Chemical Co., Rockford, IL) using BSA as a standard.

In some experiments, membrane proteins were treated with glycerol-free, recombinant N-glycanase (Genzyme Corp., Cambridge, MA) before electrophoresis. Membrane aliquots (40 μg protein) were denatured in 0.5% SDS, 50 mM β-mercaptoethanol before incubation for 22 h at 37°C in 75 μl containing N-glycanase (1 unit), 0.2% (w/v) SDS, 1.3% NP40, 150 mM sodium phosphate (pH 7.5), and 10 mM 1,10 phenanthroline. The samples were precipitated with ethanol (−20°C) before analysis by SDS-PAGE immunoblot.

*Table I. Estimation of CHIP28 Concentrations in Membranes by Dilutional Immunoblotting**

Source of membranes	CHIP28, Percent of total protein
Human red cell membranes	2.4%
Rat red cell membranes	3.7%
Rat cortex, total membranes	0.88%
Rat cortex, brush border	3.8%

* Estimates were obtained from signals of serial dilutions of cell membranes compared to dilutions of pure CHIP28 protein standard on immunoblots reacted with anti-CHIP28 (see Methods).

Electrophoresis and Immunoblotting of Membranes

SDS-PAGE was performed using the buffers described by Laemmli (1970) and 0.1 × 7 × 9 cm mini-slabs of 12% acrylamide. The gel slabs were either stained with Coomassie brilliant blue or silver reagent (Bio-Rad Laboratories). Immunoblotting was performed as described by Davis and Bennett (1984) using anti-CHIP28 or anti-N-peptide. Similar results were obtained when immunoblots were visualized with ^{125}I-protein A or enhanced chemiluminescence (Amersham Corp., Arlington Heights, IL).

Quantitative immunoblotting was performed on membranes from human and rat red cells and total membranes and brush border membrane vesicles prepared from rat renal cortex. The following samples were analyzed in adjacent lanes of a 0.15 × 14 × 16 cm SDS-PAGE slab of 12% acrylamide which was blot transferred onto nitrocellulose, incubated with anti-CHIP28 (0.01 μg/ml), and visualized with chemiluminescence: purified CHIP28 protein standard (24, 73, 240, and 730 ng/lane); human and rat red cell membranes, and brush border from rat kidney cortex (0.48, 1.6, and 4.8 μg/lane); and total membranes from rat kidney cortex (1.6, 4.8, and 16 μg/lane). Signal intensities over the M_r 28 kD region were determined by densitometry and confirmed by manual measurement of signal area. Signal was plotted vs protein concentration, and mid points of the profiles were then normalized to pure CHIP28 standard. Quantitation by this technique was previously demonstrated (Denker et al., 1988).

Preparation of Tissues for Immunolocalization of CHIP28

Wistar rats of 150 gm (Moellegaarden, Copenhagen, DK) were allowed free access to food and water before anesthesia with pentobarbital. Animals were deprived of water for 48 h before being killed in thirsting experiments. Kidneys from 20 rats were fixed by retrograde perfusion through the abdominal aorta with either 1, 2, or 8% paraformaldehyde in 0.15 M sodium cacodylate buffer (pH 7.2) or 2% paraformaldehyde plus 0.1% glutaraldehyde in 0.1 M sodium cacodylate buffer (pH 7.2). In some experiments, kidneys were perfusion-fixed with 8% paraformaldehyde in 0.1 M sodium cacodylate buffer, 0.6% NaCl, and 3% (wt/vol) dextran (T40, Pharmacia LKB Biotechnology, Inc., Piscataway, NJ). The paraformaldehyde containing fixatives were prepared from a 16% stock solution prepared 3 wk before use. Tissue blocks were prepared from the following parts of the kidney: outer cortex, inner cortex, outer stripe of outer medulla, inner stripe of outer medulla, and the transition zone between the outer and inner stripes. Blocks were also cut from sections of the inner medulla corresponding to the outer region, the middle region, and the innermost region: the papilla (represented in Fig. 1).

Blocks were further fixed by immersion for 1 h in the same fixatives, infiltrated with 2.3 M sucrose (Tokuyasu, 1986) containing 2% paraformaldehyde for 30 min, mounted on holders and rapidly frozen by stirring in liquid nitrogen.

Ultrathin cryosections were obtained with a Reichert-Jung FC 4D cryoultramicrotome at 160–180 K. Sections of 0.8 μm were placed on gelatin coated glass slides for immunohistochemistry. Sections of 70–90 nm were placed on 300 mesh Ni-grids for immunoelectron microscopy. All sections were preincubated with phosphate buffered sodium chloride containing 1% BSA and 0.05 M glycine.

Immunohistochemistry

Affinity-purified primary antibody was diluted to 0.05–0.3 μg/ml in the preincubation buffer without glycine, and the sections were incubated either for 1 h at room temperature or overnight in a humid chamber at 4°C. The sections were then washed and incubated 60 min at room temperature with peroxidase-conjugated affinity-purified goat anti-rabbit immunoglobulins at 1:100 (Dakopatts, Copenhagen, DK). The sections were again washed, and peroxidase was visualized by reaction with diaminobenzidine for 10 min, and again washed. Some of the sections were counterstained with toluidine blue or Meier staining techniques. The stained sections were analyzed with a Leitz Orthoplane microscope (E. Leitz, Inc., Rockleigh, NJ).

Immunocytochemistry

Sections for electron microscopy were incubated overnight at 4°C with primary antibody at 0.07–0.3 μg/ml before incubation for 2 h at 4°C with 10 nm protein A-gold (Janssen, Belgium). The sections were finally embedded in 2% methylcellulose containing 0.3% uranyl acetate according to Tokuyasu (1986) as modified from Griffiths et al. (1984). The sections were analyzed with a microscope (100 CX, JEOL USA, Peabody, MA).

Immunolabeling Controls

The following controls were performed and each confirmed the specificity of the immunolabelings: (*a*) incubations without primary antibody; (*b*) incubations without primary or secondary antibodies (immunohistochemistry); (*c*) incubations with primary antibody (24 ng in 80 μl) previously reacted with 1.2 μg of purified CHIP28 protein overnight at 4°C; and (*d*) incubations with preimmune serum.

Results

Characterization of Antibodies and Quantitation of Renal CHIP28

Antibodies were raised in rabbits to human red cell CHIP28 protein ("anti-CHIP28") or to a synthetic peptide corresponding to the first ten residues of the CHIP28 amino acid sequence conjugated to BSA ("anti-N-peptide"). Anti-CHIP28 is specific for the 4-kD cytoplasmic COOH-terminal domain, and anti-N-peptide is specific for the cytoplasmic NH_2 terminus (Smith and Agre, 1991). Both antibody preparations were further purified by adsorption and elution from affinity columns containing highly purified human red cell CHIP28 protein from which the M_r 40–60 kD glycosylated CHIP28 protein had been removed (see Methods).

Membranes were prepared from human red cells, rat red cells, rat renal cortex, and the apical brush border fraction of rat renal cortex (Fig. 2). When SDS-PAGE slabs were analyzed by staining with Coomassie blue or silver reagent, several protein bands became visible but not the M_r 28 kD CHIP28 or the M_r 40–60 kD glycosylated CHIP28 subunits which are known to stain poorly (Denker et al., 1988). Incubation of immunoblots containing these preparations with anti-CHIP28 or anti-N-peptide, at dilutions of <0.01 μg of IgG per ml, revealed strong, highly specific reactions over both M_r 28 kD CHIP28 and higher M_r glycosylated CHIP28 subunits (Fig. 2). As expected, after the membranes were digested with N-glycanase, specific reaction was seen only with M_r 28 kD CHIP28 protein on immunoblots incubated with anti-CHIP28 (Fig. 2) and anti-N-peptide (not shown). Similar degrees of immunoreactivity between rat and human membranes reflect the homology between murine and human CHIP28 sequences which are 94% identical (Lanahan et al., 1992).

The abundance of CHIP28 protein in each of the membranes was determined from immunoblots containing a range of dilutions of each membrane preparation and dilutions of purified CHIP28 protein standard. After incubation with anti-CHIP28, the signals of M_r 28 kD CHIP28 in membranes were normalized to the purified CHIP28 protein (Table I). Approximately 2.4% of the total human red cell membrane protein was comprised of CHIP28 protein which corresponds to approximately 200,000 copies per cell (150,000 nonglycosylated CHIP28 subunits and 50,000 glycosylated CHIP28 subunits). Almost 1% of the total protein in rat renal cortical membranes and nearly 4% of brush border protein was comprised of CHIP28.

Immunolocalization of CHIP28 in Proximal Tubules

Localization of CHIP28 in rat kidney was undertaken by incubating thin cryosections of cortex with anti-CHIP28 and histochemical reaction with conjugated peroxidase. Immunoreactivity was not detected over glomeruli. Except for the initial part of the S1 segment, strong immunoreaction was observed over all other proximal tubule segments (Fig. 3, *a*, *c*, and *d*) and was highly specific, because no reaction was noted when the antibody was previously incubated with purified CHIP28 protein (Fig. 3 *b*) or when sections were incubated with preimmune IgG (not shown). Immunoreactivity was traced down the length of the proximal tubule segments without interruption. Subsequent regions of the S1 segment, the S2 proximal convoluted segment, and S3

Figure 3. Immunohistochemical localization of CHIP28 within different renal proximal tubule segments. *a* and *b* were from cortex; *c* and *d* were from deeper cortex and outer stripe of outer medulla; *e* and *f* were from the transition between outer and inner stripes of the outer medulla. Sections were incubated with anti-CHIP28, and immunoreactions were visualized with peroxidase-conjugated goat-anti-rabbit immunoglobulin (see Methods). (*a*) Immunolabeling was not seen over glomeruli (*G*) or some S1 segment proximal tubules. (S1 segments are identified by a higher brush border than segment S2.) Other S1 segments exhibited immunoreactions over the apical brush borders. S2 segment proximal tubules all exhibited heavy immunolabeling over the apical brush borders and over basolateral membranes (*arrows*). No immunoreaction was detected over collecting ducts (*C*) or capillary endothelium. (*b*) Immunolabeling of proximal tubules was not observed when anti-CHIP28 was preadsorbed with pure CHIP28 protein. (*c*) All S3 segment proximal tubules demonstrated heavy immunoreactions over apical brush borders and basolateral membranes (*arrows*) when counterstained with Meier. (S3 segments have a high brush border and limited basolateral interdigitations.) (*d*) Tangentially sectioned S3 segment proximal tubules clearly revealed immunoreactions over basal and lateral plasma membranes (*arrows*). Collecting ducts (*C*) did not label. (*e*) The transition zone revealed a proximal tubule (*large arrow*) continuing into a descending thin limb; both exhibited immunostaining. Tubules with relatively thicker epithelium (*D*) are probably descending thin limbs from long looped nephrons. The thin walled structure (*small arrow*) is probably a short looped descending thin limb in a vascular bundle. No immunoreaction was observed over thick ascending limbs (*T*). (*f*) High magnification of a similar section demonstrated immunostaining of the abrupt transition (*arrows*) of proximal tubules (*P*) and descending thin limbs. Bars, 20 μm.

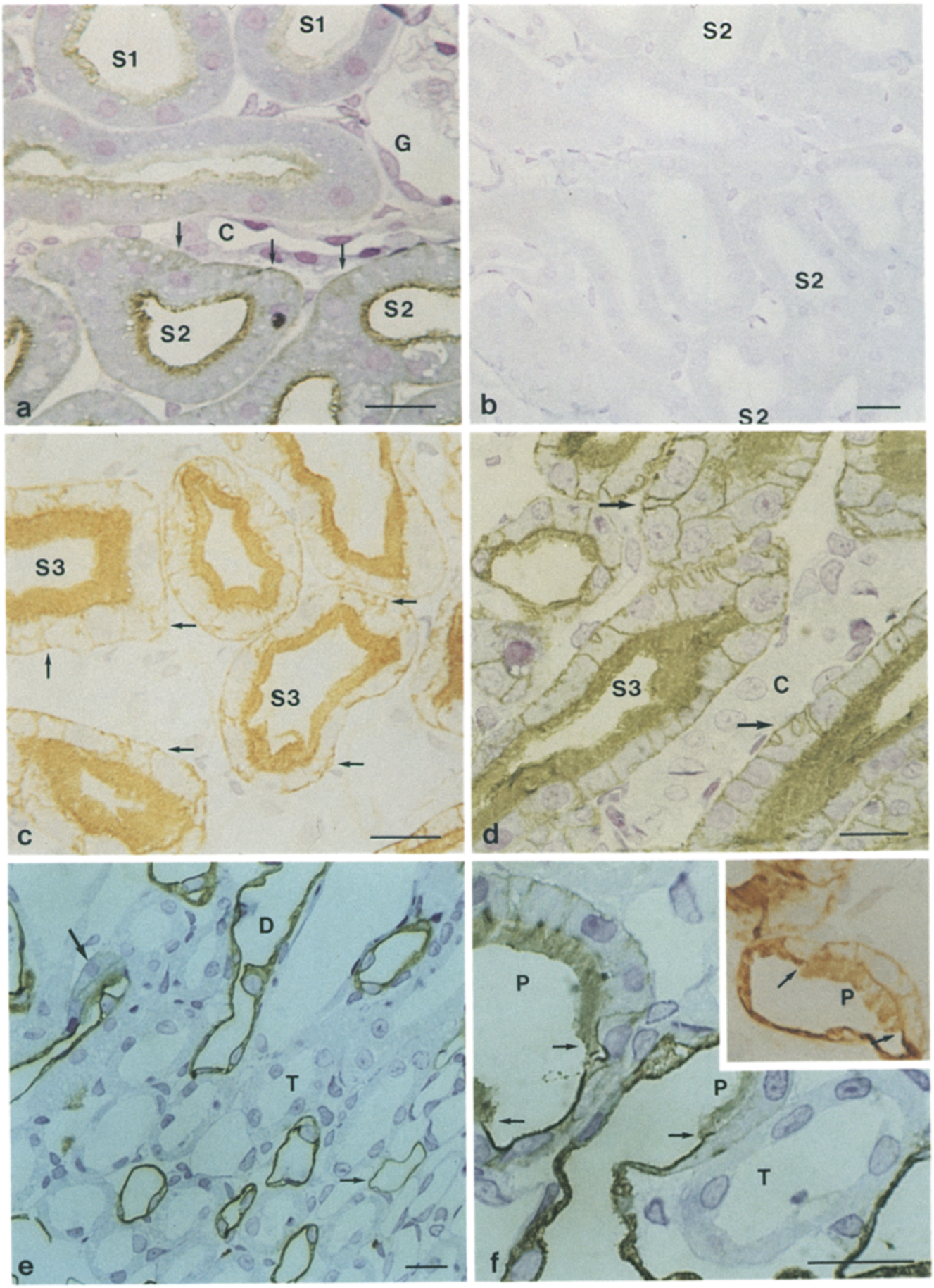
S1
S1
G
C
S2
S2
a
S2
S2
S2
b
S3
S3
c
S3
C
d
D
T
e
P
P
P
T
f

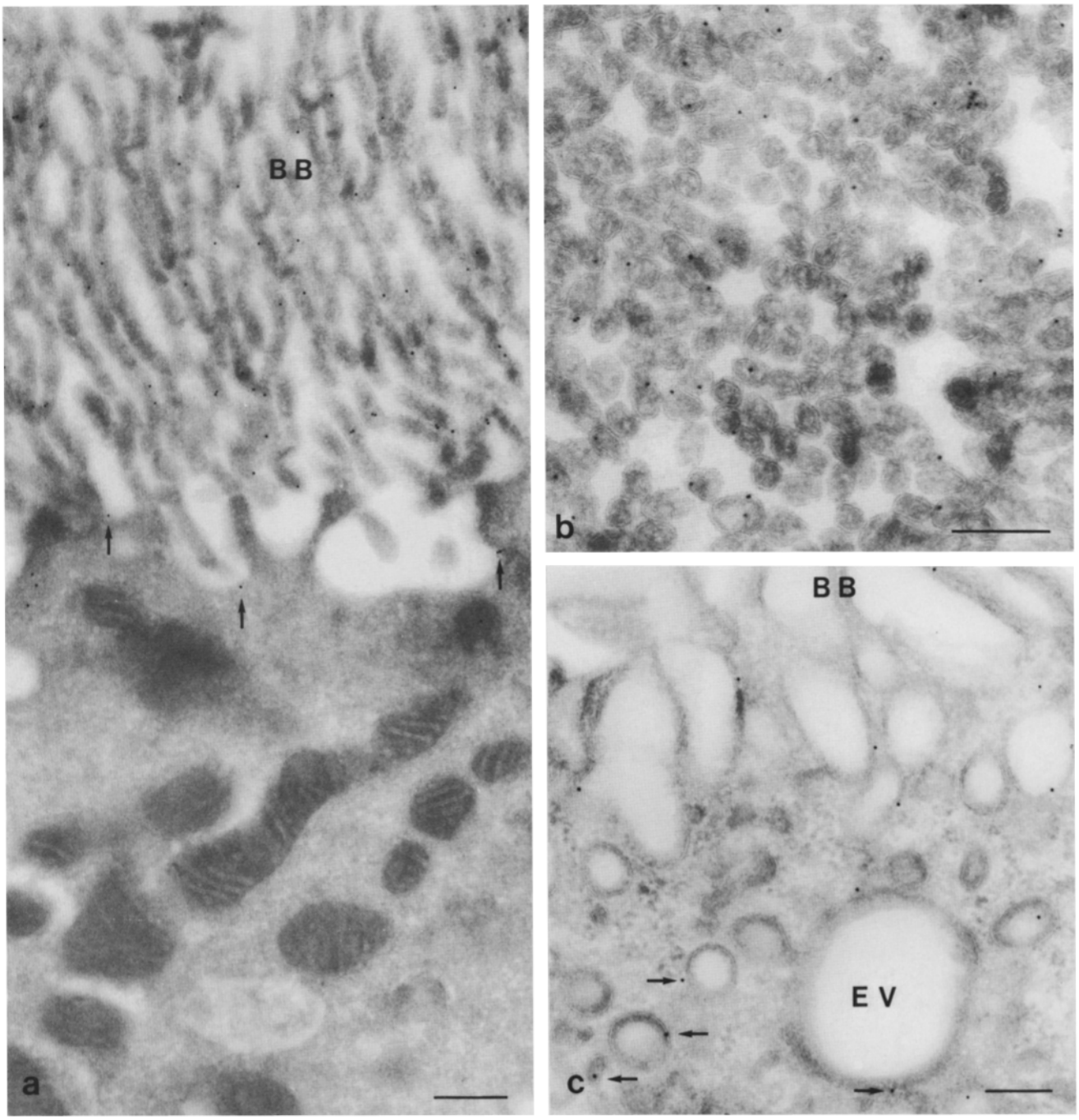

Figure 4. Subcellular localization of CHIP28 within the apical part of renal proximal tubule epithelia. Anti-CHIP28 was used with protein A-gold (see Methods). (*a*) Immunogold labeling was observed over the brush border (*BB*) and endocytic invaginations (*arrows*) of an S3 proximal tubule cell. (*b*) Immunogold labeling of cross-sectioned microvilli was confined to the cytoplasmic leaflet of the apical plasma membrane. (*c*) Only limited immunogold labeling was observed over the endocytic apparatus of an S2 proximal tubule cell, where it was located in endocytic vesicles (*EV*), vacuoles, and dense apical tubules (*arrows*). Bars, 0.3 μm.

straight tubule segment all exhibited heavy immunolabeling which extended around the lateral and basal margins of all proximal tubular epithelia (Fig. 3, *c* and *d*). Sections from outer medulla at the transition between distal segments of proximal tubules (S3) and initial segments of descending thin limbs (DTL1 and DTL2) also demonstrated that CHIP28 immunoreactivity was specific and was not interrupted (Fig. 3, *e* and *f*).

Subcellular localization of CHIP28 was undertaken by immunoelectron microscopy of ultrathin cryosections incu-

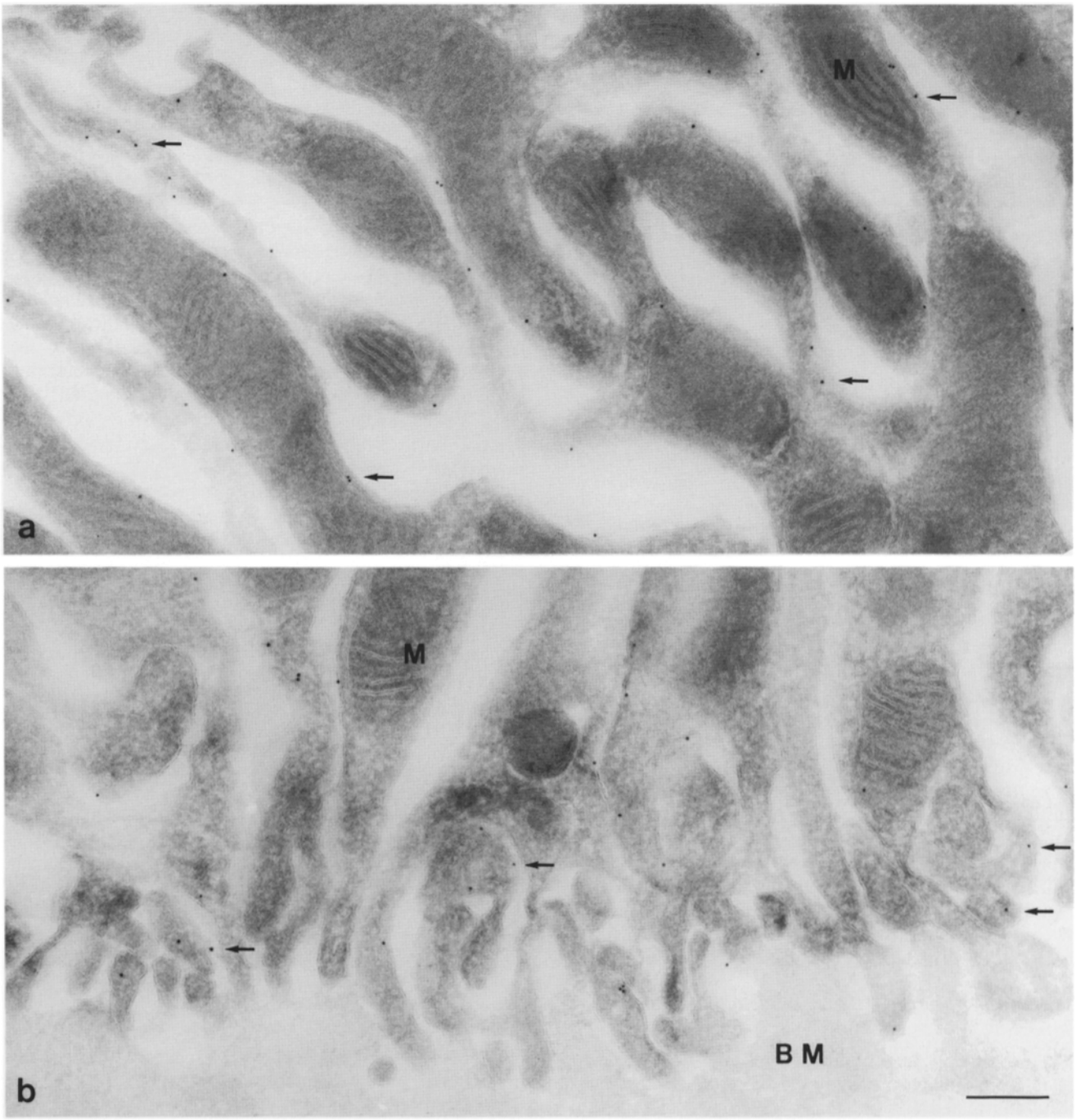

Figure 5. Subcellular localization of CHIP28 within the basal part of renal proximal tubule epithelia. (*a*) Anti-CHIP28-immunogold labeling was evenly distributed along the lateral plasma membrane of an S2 proximal tubule (*arrows*). (*b*) Section of the basal part of an S1 proximal tubule demonstrated immunogold labeling over the plasma membranes of basal villi (*arrows*) and lateral plasma membranes but not over mitochondria (*M*) or the basement membrane (*BM*). Bars, 0.3 μm.

bated with anti-CHIP28 and decorated with protein A conjugated to 10 nM gold particles (Figs. 4 and 5). Proximal tubular epithelia exhibited strong immunoreactivity over the apical brush border. Microvilli appeared to be evenly stained along their entire length including the most distal parts (Fig. 4 *a*). Analysis of cross-sections of brush border microvilli confirmed immunolocalization at the inner surface of the plasma membrane (Fig. 4 *b*), consistent with reaction of anti-CHIP28 with the COOH-terminal cytoplasmic domain of the molecule. Only minimal staining of endocytic vesicles and vacuoles as well as of dense apical tubules was noted within the cell body (Fig. 4 *c*), and no other subcellular com-

ponents were labeled. Analysis of the lateral and basal plasma membranes of proximal tubules also revealed specific immunostaining (Fig. 5). Thus, CHIP28 exists in both apical and basolateral proximal tubule plasma membranes, and both are known to exhibit constitutively high osmotic water permeability (Fig. 1).

Immunolocalization of CHIP28 in Descending Thin Limbs

Sections from outer and inner renal medulla were incubated with CHIP28 antibodies. Light microscopic evaluation (Fig. 6) revealed heavy anti-CHIP28 immunostaining of descending thin limbs, including segments of short loops and long loops of Henle. Anti-N-peptide gave a weaker immunoreaction, but the localization was otherwise identical to that found with anti-CHIP28 both in proximal tubules (not shown) and in descending thin limbs (Fig. 6 *d*). As with the proximal tubule, immunoreactivity was found over both apical and basolateral margins of descending thin limb epithelia which was readily observed in areas around the nucleus (Fig. 6 *b*). CHIP28 immunoreactivity was not interrupted down the length of the descending thin limbs until the transition at the turn of the loop of Henle where immunoreactive epithelia join non-reactive epithelia (Fig. 6 *f*). Approximately half of thin limbs in the inner medulla failed to react with anti-CHIP28 (Fig. 6 *e*). Subsequent electron microscopic analysis showed that these are ascending thin limbs (see below).

Electron microscopic analyses of outer and inner medulla were also performed with anti-CHIP28 and revealed heavy immunolabeling of all descending thin limb segments (Figs. 7 and 8), including short and long loops of Henle. As seen in the proximal tubules, CHIP28 subcellular localization was confined to apical and basolateral membranes of descending thin limbs (Figs. 7 and 8). Moreover, electron microscopy identified that the nonreactive thin limbs were ascending thin limbs (Fig. 7 *e*). Thus, CHIP28 was found in apical and basolateral membranes of descending thin limbs, which are both known to be highly permeable to water, but CHIP28 was not detected in ascending thin limbs which are highly impermeable to water (Fig. 1).

Lack of Identifiable CHIP28 in Distal Nephron and Collecting Ducts

Sections through renal cortex and medulla were inspected for CHIP28 immunoreactivity over thick ascending limbs, distal convoluted tubules, and connecting tubules. No immunoreactions were detected either by light microscopy (Figs. 3 and 6) or by immunoelectron microscopy with anti-CHIP28 or anti-N-peptide (Fig. 8). These structures are known to have negligible water permeability (Fig. 1).

Collecting ducts in cortex, outer medulla, and inner medulla were also studied with light and immunoelectron microscopy. The apical membranes of collecting duct epithelia are known to have only modest basal levels of water permeability (Fig. 1), and no immunolabeling was noted in sections from normal rat kidneys (Figs. 3–8). Thirsted rats are known to have high circulating ADH levels and maximally concentrated urine, conditions known to confer a high level of water permeability to these collecting ducts (Fig. 1). Nevertheless, collecting ducts from thirsted rats failed to react with either anti-CHIP28 or anti-N-peptide (not shown) indicating that ADH regulated water channels are not recognized by the CHIP28 antibodies. Basolateral membranes from collecting ducts did not label by immunoreaction with anti-CHIP28 (Figs. 3, 6, 8, *b* and *c*) or anti-N-peptide (Fig. 6 *d*), indicating that the constitutively high basolateral collecting duct water permeability is not due to CHIP28.

Capillary endothelia within the vasa recta were also analyzed with immunoelectron microscopy. No significant staining of capillary endothelial cells was detected (Figs. 7 *c* and 8 *d*).

Discussion

The discovery of CHIP28 has provided fortuitous molecular insight into the mechanism by which kidneys reabsorb water. CHIP28 was first noted as a contaminant in purifications of Rh protein from red cells (Agre et al., 1987; Saboori et al., 1988) and a similar protein was identified in renal tubules during screening of autopsy specimens (Denker et al., 1988). The idea that CHIP28 may be a water channel emerged when the amino acid sequence of CHIP28 was found to contain homologies with a family of putative membrane channels from diverse sources including the roots of plants (Smith and Agre, 1991; Preston and Agre, 1991). Two experiments ultimately demonstrated that CHIP28 is a water channel. First, expression of CHIP28 conferred *Xenopus* oocytes with enhanced osmotic water permeability (Preston et al., 1992). Second, reconstitution of purified red cell CHIP28 into synthetic liposomes provided direct biophysical demonstration of water-selective channel activity with unit water permeability sufficient to account for most red cell water transport (Zeidel et al., 1992). The structural similarity of red cell and renal CHIP28 predicts that their functions

Figure 6. Immunohistochemical localization of CHIP28 within different tubule segments in renal medulla. Sections from the inner stripe of outer medulla (*a–d*) and inner medulla (*e, f*), were incubated with anti-CHIP28 (*a, b, e, f*), preadsorbed anti-CHIP28 (*c*), or anti-N-peptide (*d*) (see Methods). (*a*) Immunolabeling was demonstrated over descending thin limbs (*D*) but not over thick ascending limbs (*T*) or collecting ducts (*C*). A red cell (*arrow*) was located within an unlabeled capillary (see also *d*). (*b*) Higher magnification of descending thin limbs (*D*) demonstrated immunoreactions over both apical and basal membranes which was especially apparent around nuclei (*arrows*). (*c*) No immunostaining was observed when anti-CHIP28 was preadsorbed with pure CHIP28 protein. (*d*) Incubation of sections with anti-N-peptide revealed immunoreactions qualitatively similar to anti-CHIP28. (*e*) At the level of mid inner medulla, most descending thin limbs (*D*) were immunostained around their entire circumference. Several thin walled structures (*arrows*) and collecting duct epithelia (*C*) were not labeled. (*f*) At the innermost level of the medulla (the papilla) where descending thin limbs (*D*) join ascending thin limbs, immunolabeling around the tubule circumference was incomplete (*arrows*) with abrupt transitions between immunolabeled and unlabeled cells. Papillary collecting ducts were not immunostained (*C*). Bars, 20 μm.

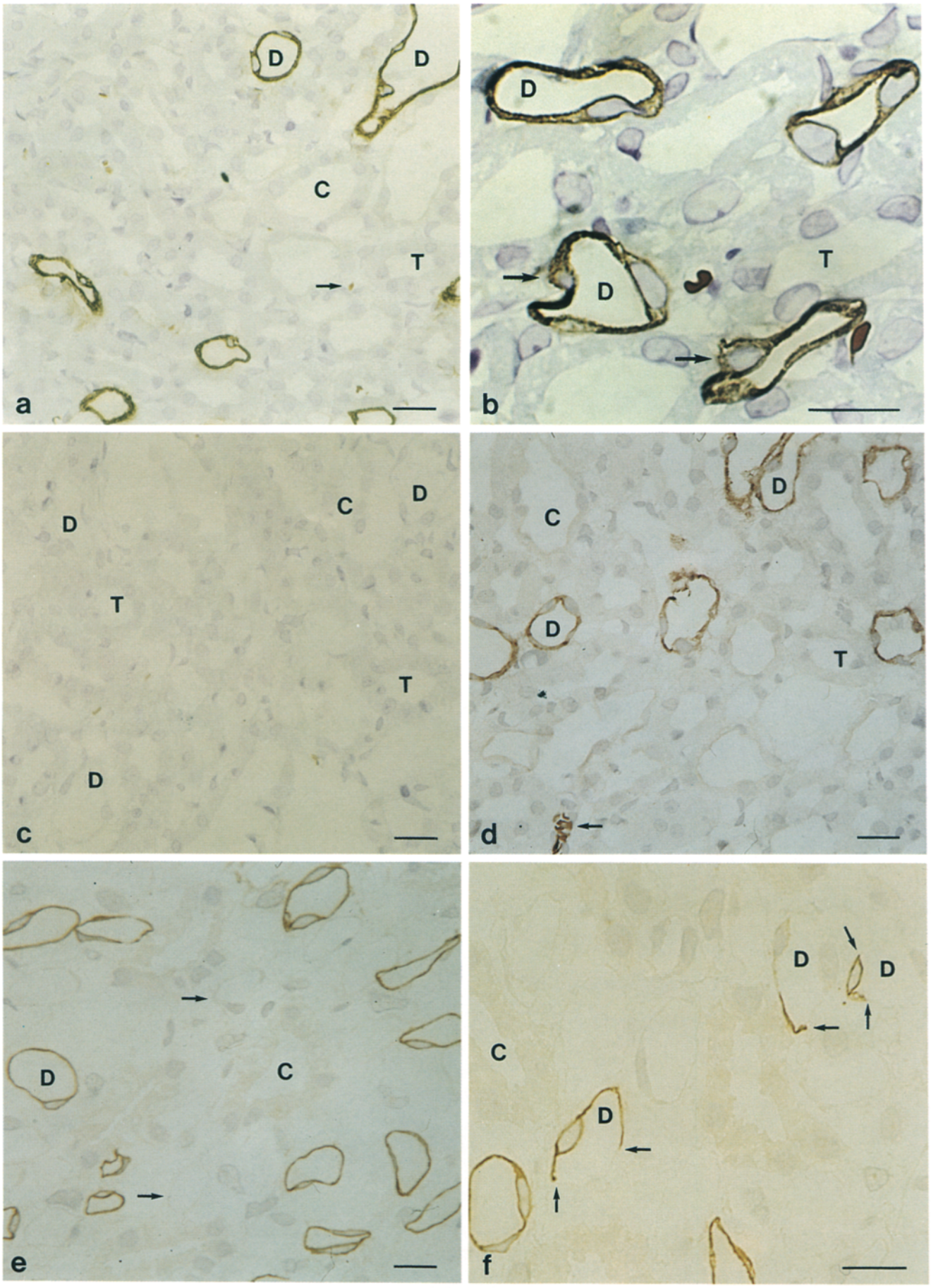
D
D
C
T
a
D
T
D
b
C
D
D
T
T
D
c
C
D
D
T
d
D
D
C
D
e
C
D
D
C
D
f

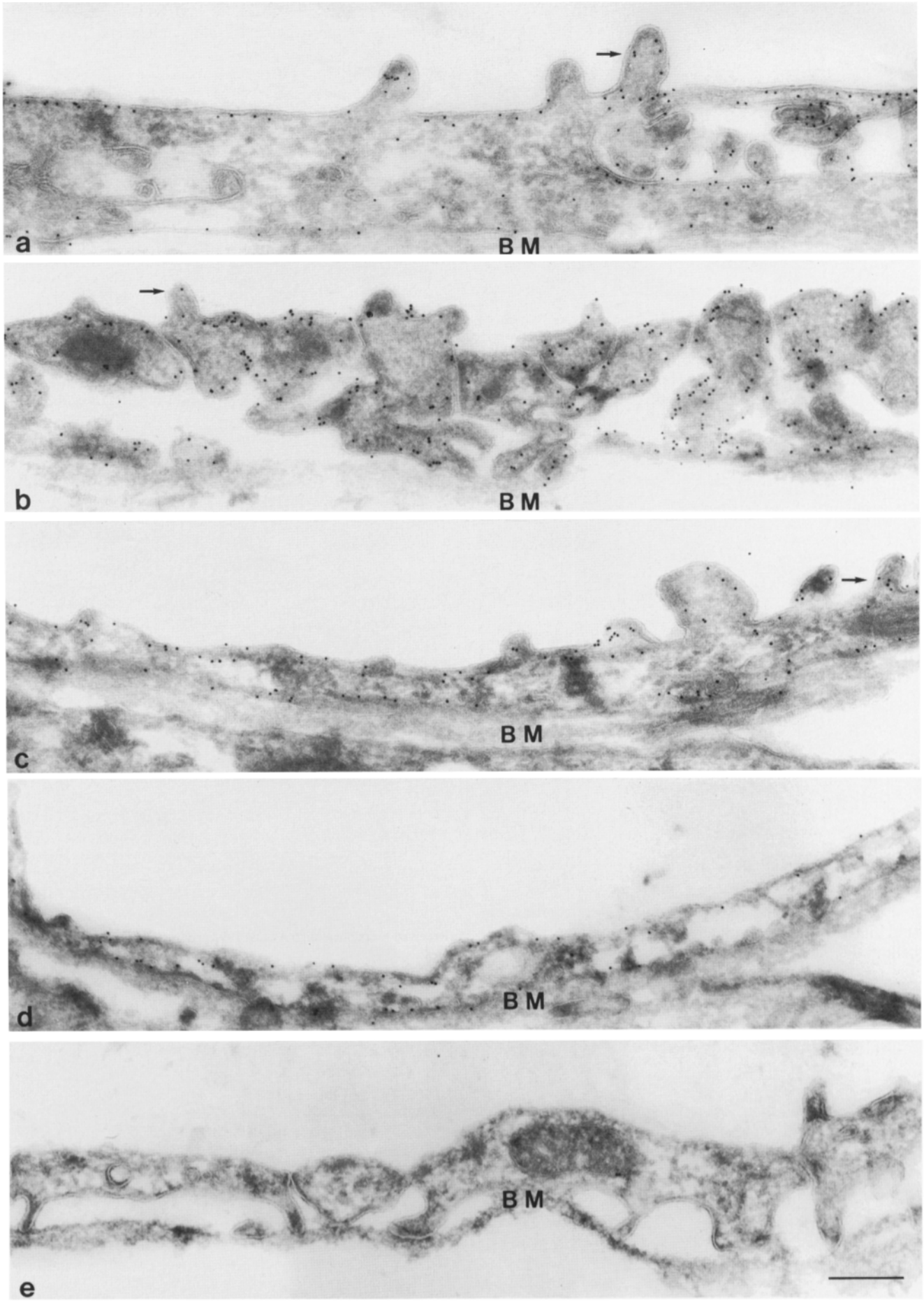
a
BM
b
BM
c
BM
d
BM
e
BM

are also related. The nonglycosylated red cell and kidney CHIP28 subunits had identical electrophoretic mobilities of M_r 28 kD. The glycosylated rat cell and rat renal CHIP28 molecules exhibited apparent electrophoretic mobilities of M_r 33–50 kD and M_r 33–40 kD, but it is unclear if this reflects inherent differences within the glycan structures or if the red cell glycosylated CHIP28 subunits bear one or two glycans while the renal subunits bear only one. After N-glycanase digestion, rat red cell and renal CHIP28 proteins had identical electrophoretic mobilities and exhibited identical reactions with CHIP28 antibodies recognizing epitopes at the opposite ends of the molecule. Thus, all evidence suggests that the core polypeptides in red cell and renal CHIP28 molecules are the same.

Large volumes of water are filtered across the mammalian renal glomerulus, amounting to at least ten times the extracellular fluid volume per day. Of this, 80–90% is reabsorbed osmotically by the combination of the proximal tubule and the descending limb of Henle's loop, both of which possess constitutively high osmotic water permeabilities (Fig. 1). Water reabsorption from the descending limb also plays a vital role in the countercurrent multiplication process that concentrates the urine (Knepper and Rector, 1991). The studies reported here strongly support the hypothesis that the CHIP28 water channel is responsible for the high osmotic water permeability of the proximal tubule and descending limb. CHIP28 was found to be present in large amounts in both the apical and basolateral membranes of these cells, and it comprised nearly 4% of the total protein in brush border membrane vesicles. Given such abundance and its large unit water permeability, CHIP28 could provide the capacity needed to reabsorb the massive volumes of filtrate which pass through the glomerulus, although the existence of paracellular water pathways cannot be excluded (Whittembury and Reuss, 1992). Therefore, we propose that CHIP28 is a major water channel of the renal proximal tubules and descending thin limbs if not the exclusive water channel at these locations.

The presence of CHIP28 at the apical and along the lateral and basal membranes of polarized epithelia implicates this protein in transcellular water flow. CHIP28 apparently mediates uptake of water at the apical membrane and exit of water from basolateral membranes, with the direction of water movement following the osmotic gradient created by energy-dependent ion transporters. Most membrane transporters exist at either apical or basolateral locations in polarized epithelium (reviewed by Rodriguez-Boulan and Nelson, 1989), so existence of CHIP28 proteins at both locations is very atypical. The lack of significant amounts of intracellular CHIP28 suggests that it is not actively cycled by endocytosis and therefore differs from H^+ATPase and other renal transporters (reviewed by Brown, 1989). The amount of CHIP28 in basolateral membranes of proximal tubules was not quantitated biochemically, but it appeared less abundant than in the apical brush borders by both light and immunoelectron microscopy. It is not known whether this may reflect differences in labeling efficiency due to antibody penetration or actual protein abundance. It is also not known what path water takes as it passes through tubular epithelial cells, so it is unclear if the points of exit need water channels in the same quantity and organization as the intake channels, or if other water channel isoforms may also exist. The abundance of CHIP28 appeared about equal in apical and basolateral membranes of descending thin limbs.

While the cellular and subcellular distribution of CHIP28 is now defined in the kidney, this report has raised several new questions. The lack of detectable CHIP28 within collecting ducts in normal and thirsted rats demonstrated that CHIP28 is distinct from the ADH-regulated water channel. The molecular identity of the ADH-water channel therefore remains unknown, but the possibility that it is genetically related to CHIP28 is intriguing and may provide an approach to its molecular identification. Our preliminary studies indicate that CHIP28 may exist in several nonrenal tissues of the body, and if confirmed, analysis of the structural organization may provide molecular insight into other possible functions of CHIP28. It is also not clear what functions are played by the homologs of CHIP28 in microbial and plant tissues, and definition of the cellular and subcellular distribution of these CHIP28 homologs may therefore provide molecular clues to the basic biological phenomenon of osmotic water movement.

The authors thank I. Kristoffersen, H. Sidelmann, and A. Meier for excellent technical assistance, and Dr. Ray Pratt for brush border membrane vesicles and helpful suggestions.

Support for this study was provided by the Danish Medical Research Council, the Biomembrane Research Center of the University of Aarhus, the University of Aarhus Research Foundation, Novo Foundation, and the National Heart, Lung, and Blood Institute of the National Institutes of Health. P. Agre is an Established Investigator of the American Heart Association.

Received for publication 6 August 1992 and in revised form 30 September 1992.

Figure 7. Subcellular localization of CHIP28 within descending thin limbs (*DTL*) at different levels of renal medulla. Sections from outer medulla (*a* and *b*) or inner medulla (*c–e*) were incubated with anti-CHIP28. (*a*) Immunogold labeling was restricted to the cytoplasmic leaflets of apical plasma membranes, including projecting microvilli (*arrow*), and basolateral plasma membranes of DTL1 epithelia from short looped nephrons. (DTL1 is characterized by few microvilli and few tight junctions.) (*b*) High density immunogold labeling was observed at these locations and in basolateral infoldings in DTL2 epithelium from long looped nephrons. (DTL2 is characterized by several tight junctions and extensive basolateral infolding.) (*c* and *d*) Immunogold labeling was observed at these locations in DTL3 epithelia from the initial level of inner medulla (*c*) and in the papilla (*d*). (DTL3 is characterized by few microvilli or junctions and limited basolateral infolding.) (*f*) No immunogold labeling was observed over ascending thin limb epithelia (identified by the presence of very few microvilli and several tight junctions). No immunogold labeling was observed over basement membranes in any segment (*BM*) or over capillary endothelial cells (*c*). Bars, 0.3 μm.

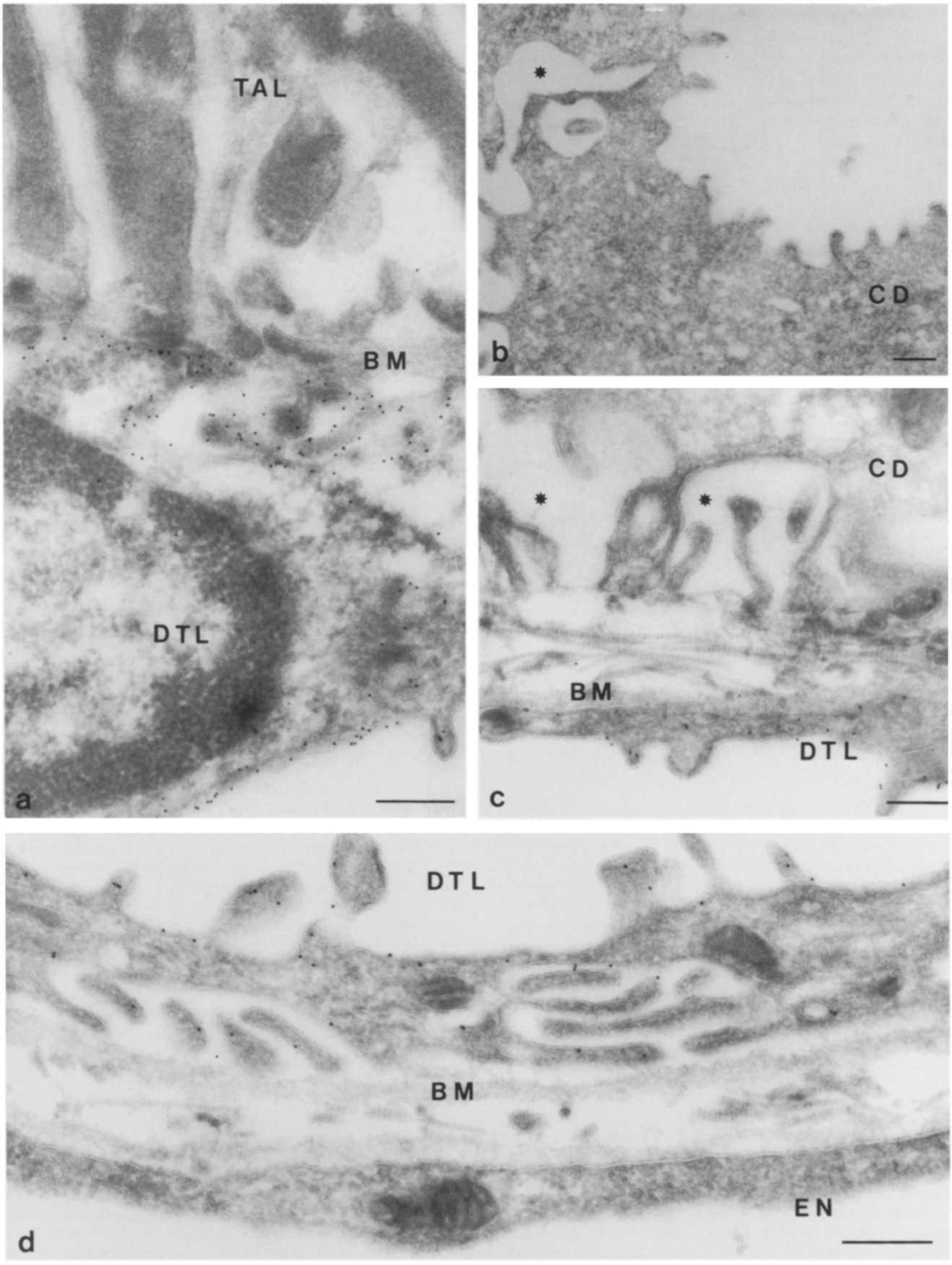
TAL
BM
DTL
a
CD
b
CD
BM
DTL
c
DTL
BM
EN
d

References

Agre, P., A. M. Saboori, A. Asimos, and B. L. Smith. 1987. Purification and partial characterization of the M_r 30,000 integral membrane protein associated with the erythrocyte Rh(D) antigen. *J. Biol. Chem.* 262:17497–17503.

Bennett, V. 1983. Proteins involved in the membrane-cytoskeleton association in human erythrocytes: spectrin, ankyrin and band 3. *Methods Enzymol.* 96:313–324.

Brown, D. 1989. Membrane recycling and epithelial cell function. *Am. J. Physiol.* 256:F1–F12.

Brown, D. 1991. Structural-functional features of antidiuretic hormone-induced water transport in the collecting duct. *Seminars Nephrol.* 11:478–501.

Burg, M. B., and N. Green. 1973. Function of the thick ascending limb of Henle's loop. *Am. J. Physiol.* 224:659–668.

Chou, C.-L., J. M. Sands, H. Nonoguchi, and M. A. Knepper. 1990. Urea gradient-associated fluid absorption with $\sigma_{urea} = 1$ in rat terminal collecting duct. *Am. J. Physiol.* 258:F1173–F1180.

Chou, C.-L., and M. A. Knepper. 1992. In vitro perfusion of chinchilla thin limb segments: segmentation and osmotic water permeability. *Am. J. Physiol.* 263:F417–F426.

Davis, J. Q., and V. Bennett. 1984. Brain ankyrin: purification of a 72,000 M_r spectrin-binding domain. *J. Biol. Chem.* 259:1874–1881.

Denker, B. M., B. L. Smith, F. P. Kuhajda, and P. Agre. 1988. Identification, purification, and partial characterization of a novel M_r 28,000 integral membrane protein from erythrocytes and renal tubules. *J. Biol. Chem.* 263:15634–15642.

Finkelstein, A. 1987. Water Movement Through Lipid Bilayers, Pores, and Plasma Membranes, Theory and Reality. John Wiley and Sons, Inc., New York. 228 pp.

Gorin, M. B., S. B. Yancey, J. Cline, J.-P. Revel, and J. Horwitz. 1984. The major intrinsic protein (MIP) of the bovine lens fiber membrane: characterization and structure based on cDNA cloning. *Cell.* 39:49–59.

Green, R., and G. Giebisch. 1989. Reflection coefficients and water permeability in rat proximal tubule. *Am. J. Physiol.* 257:F658–F668.

Griffiths, G., A. McDowall, R. Back, and J. Dubochet. 1984. On the preparation of cryosections for immunocytochemistry. *J. Ultrastruct. Res.* 89: 65–78.

Gross, J. B., and J. P. Kokko. 1975. A functional comparison of the cortical collecting tubule and the distal convoluted tubule. *J. Clin. Invest.* 55:1284–1294.

Handler, J. S. 1988. Antidiuretic hormone moves membranes. *Am. J. Phys.* 255:F375–F382.

Harris, H. W., K. Strange, and M. L. Zeidel. 1991. Current understanding of the cellular biology and molecular structure of the antidiuretic hormone-stimulated water transport pathway. *J. Clin. Invest.* 88:1–8.

Horster, M. S., and H. Zink. 1982. Functional differentiation of the medullary collection duct: influence of vasopressin. *Kidney Int.* 22:360–365.

Imai, M. 1979. Connecting tubule: functional subdivision of the rabbit distal nephron segment. *Kidney Int.* 15:346–356.

Imai, M. 1984. Functional heterogeneity of the descending limbs of Henle's loops. II. Interspecies differences among rabbits, rats, and hamsters. *Pflügers Arch. Eur. J. Physiol.* 402:393–401.

Knepper, M. A., and F. C. Rector, Jr. 1991. Urinary concentration and dilution. *In* The Kidney, 4th edition. B. M. Brenner, and F. C. Rector, Jr., editors. W. B. Saunders, Philadelphia. 445–482.

Laemmli, U. K. 1970. Cleavage of structural proteins during the assembly of the head of bacteriophage T4. *Nature (Lond.).* 227:680–685.

Lanahan, A., J. B. Williams, L. K. Sanders, and D. Nathans. 1992. Growth factor-induced delayed early response genes. *Mol. Cell Biol.* In press.

Lankford, S. P., C.-L. Chou, Y. Terada, S. M. Wall, J. B. Wade, and M. A. Knepper. 1991. Regulation of collecting duct water permeability independent of cAMP-mediated AVP response. *Am. J. Physiol.* 261:F554–F566.

Mürer, H., and P. Gmaj. 1986. Transport studies in plasma membrane vesicles isolated from renal cortex. *Kidney Int.* 30:171–186.

Preston, G. M., and P. Agre. 1991. Isolation of the cDNA for erythrocyte integral membrane protein of 28 kilodaltons: Member of an ancient channel family. *Proc. Natl. Acad. Sci. USA.* 88:11110–11114.

Preston, G. M., T. P. Carroll, W. B. Guggino, and P. Agre. 1992. Appearance of water channels in *Xenopus* oocytes expressing red cell CHIP28 protein. *Science (Wash. DC).* 256:385–387.

Reif, M. C., S. L. Troutman, and J. A. Schafer. 1984. Sustained response to vasopressin in isolated rat cortical collecting tubule. *Kidney Int.* 26:725–732.

Rocha, A. S., and J. P. Kokko. 1973. Sodium chloride and water transport in the medullary thick ascending limb of Henle. *J. Clin. Invest.* 52:612–623.

Rodriquez-Boulan, E., and W. J. Nelson. 1989. Morphogenesis of the polarized epithelial cell phenotype. *Science (Wash. DC).* 245:718–725.

Saboori, A. M., B. L. Smith, and P. Agre. 1988. Polymorphism in the M_r 32,000 Rh protein purified from Rh(D)-positive and -negative erythrocytes. *Proc. Natl. Acad. Sci. USA.* 85:4042–4045.

Schafer, J. A., C. S. Patlak, S. L. Troutman, and T. E. Andreoli. 1978. Volume reabsorption in the pars recta. II. Hydraulic conductivity coefficient. *Am. J. Physiol.* 234:F340–F348.

Smith, B. L., and P. Agre. 1991. Erythrocyte M_r 28,000 Transmembrane protein exists as a multisubunit oligomer similar to channel proteins. *J. Biol. Chem.* 266:6407–6415.

Tokuyasu, K. T. 1986. Application of cryoultramicrotomy to immunocytochemistry. *J. Microsc.* 143:139–149.

Verkman, A. S. 1989. Mechanisms and regulation of water permeability in renal epithelia. *Am. J. Physiol.* 257:C837–C850.

Whittembury, G., and L. Reuss. 1992. Mechanisms of coupling of solute and solvent transport in epithelia. *In* The Kidney: Physiology and Pathophysiology. D. W. Seldin and G. Giebisch, editors. Raven Press, New York. 317–360.

Zeidel, M. L., S. V. Ambudkar, B. L. Smith, and P. Agre. 1992. Reconstitution of functional water channels in liposomes containing purified red cell CHIP28 protein. *Biochemistry.* 31:7436–7440.

Figure 8. Lack of subcellular localization of CHIP28 within renal thick ascending limbs or collecting ducts with anti-CHIP28. (*a*) No immunogold labeling of thick ascending limbs (*TAL*) was noted, whereas adjacent descending thin limbs (*DTL*) exhibited distinct immunoreactions. (*b*) No immunogold labeling was observed over the apical plasma membrane or other apical parts of collecting duct epithelia (*CD*) in inner medulla. Furthermore, no labeling was observed over basolateral collecting duct membranes (*asterisk*). (*c*) No immunogold labeling was observed over basal plasma membrane infoldings around intercellular spaces (*asterisks*) within collecting duct epithelia (*CD*) from outer medulla. In contrast, adjacent descending thin limbs (*DTL*) exhibited specific immunogold labeling. (*d*) Immunogold labeling of descending thin limb epithelia (*DTL*) was observed with anti-N-peptide. Bars, 0.3 μm.